



OPEN ACCESS

EDITED BY

Xiaoxin Wang,
Georgetown University Medical Center,
United States

REVIEWED BY

Komuraiah Myakala,
Georgetown University, United States
Jian Li,
Hunan Normal University, China
Lin Chen,
Northwest University, China

*CORRESPONDENCE

Feng Lin,
✉ lf0237@gzucm.edu.cn
Guoliang Xiong,
✉ szxiongguoliang@126.com

[†]These authors have contributed equally
to this work and share first authorship

SPECIALTY SECTION

This article was submitted to
Renal Pharmacology,
a section of the journal
Frontiers in Pharmacology

RECEIVED 20 November 2022

ACCEPTED 22 March 2023

PUBLISHED 06 April 2023

CITATION

Lu L, Lu J, Chen J, Wang B, Peng H,
Peng J, Liu X, Lin F and Xiong G (2023),
Biomarker identification and pathway
analysis of *Astragalus membranaceus* and
Curcuma zedoaria couplet medicines on
adenine-induced chronic kidney disease
in rats based on metabolomics.
Front. Pharmacol. 14:1103527.
doi: 10.3389/fphar.2023.1103527

COPYRIGHT

© 2023 Lu, Lu, Chen, Wang, Peng, Peng,
Liu, Lin and Xiong. This is an open-access
article distributed under the terms of the
[Creative Commons Attribution License
\(CC BY\)](https://creativecommons.org/licenses/by/4.0/). The use, distribution or
reproduction in other forums is
permitted, provided the original author(s)
and the copyright owner(s) are credited
and that the original publication in this
journal is cited, in accordance with
accepted academic practice. No use,
distribution or reproduction is permitted
which does not comply with these terms.

Biomarker identification and pathway analysis of *Astragalus membranaceus* and *Curcuma zedoaria* couplet medicines on adenine-induced chronic kidney disease in rats based on metabolomics

Lingfei Lu^{1,2†}, Jiandong Lu^{3†}, Jiwei Chen^{1,2}, Bing Wang³,
Hongcheng Peng^{1,2}, Jinting Peng⁴, Xinhui Liu¹, Feng Lin^{5*} and
Guoliang Xiong^{1*}

¹Department of Nephrology, Shenzhen Traditional Chinese Medicine Hospital, Guangzhou University of Chinese Medicine, Shenzhen, Guangdong, China, ²The Fourth Clinical Medical College of Guangzhou University of Chinese Medicine, Shenzhen, Guangdong, China, ³Department of Nephrology, Shenzhen Traditional Chinese Medicine Hospital Nanjing University of Chinese Medicine, Shenzhen, China, ⁴Department of Gynecology, Shenzhen Traditional Chinese Medicine Hospital, Guangzhou University of Chinese Medicine, Shenzhen, Guangdong, China, ⁵Department of Urology, Shenzhen Traditional Chinese Medicine Hospital Guangzhou University of Chinese Medicine, Shenzhen, Guangdong, China

Background: Chronic kidney disease (CKD) is usually insidious, and most affected individuals are asymptomatic until the disease becomes advanced. The effective treatment of CKD would rely on the incorporation of multidisciplinary approaches. *Astragalus membranaceus* (AM) and *Curcuma zedoaria* (CZ) have been widely used in the treatment of CKD. However, the mechanism of AM and CZ in the treatment of CKD is still unclear.

Methods: This study was designed to evaluate the effects of AM and CZ on adenine-induced rats and to investigate the underlying mechanism by using metabolomic analysis. Addition of 0.75% adenine to the diet of rats for 3 weeks induced the animal model of CKD. The rats in the treatment group were treated with AM and CZ (2.1g/kg/day) for 4 weeks. Blood and kidney samples were collected for biochemical and histological examination. Ultra-high-performance liquid chromatography/Q Exactive HFX mass spectrometer (UHPLC-QE-MS) was applied to analyze metabolic profiling variations in the kidney.

Abbreviations: ACEI, angiotensin converting enzyme inhibitor; AM, *Astragalus membranaceus*; ARB, angiotensin receptor blocker; BUN, blood urea nitrogen; CKD, chronic kidney disease; CZ, *Curcuma zedoaria*; ESI, electrospray ionization; NAD⁺, nicotinamide adenine dinucleotide; NADP, nicotinamide adenine dinucleotide phosphate; NO, nitric oxide; NOS, nitric oxide synthetase; OPLS-DA, orthogonal partial least squares discriminant analysis; PCA, principal component analysis; QC, quality control; SCR, serum creatinine; SGLT2, sodium-glucose cotransporter 2; TCM, traditional chinese medicine; UHPLC-MS/MS, ultra-high-performance liquid chromatography-tandem mass spectrometry; VIP, variable importance in the projection.

Results: The results showed that AM and CZ could significantly reduce serum creatinine (Scr) and blood urea nitrogen (BUN) levels in CKD rats and alleviate renal pathological injury. By comparing the endogenous components of the normal group and the model group in positive ion mode and negative ion mode, a total of 365 and 155 different metabolites were screened, respectively. A total of 117 and 73 metabolites with significantly different expressions were identified between model group and AM and CZ group in positive ion mode and negative ion mode, respectively. The pivotal pathways affected by AM and CZ included nicotinate and nicotinamide metabolism, and glycine, serine and threonine metabolism. Furthermore, significant changes in metabolites in CKD rats after AM and CZ therapies were observed, including L-Threonine, D-pantothenic acid, and nicotinamide. Moreover, we found that AM and CZ significantly reduced renal fibrosis and inflammation in CKD rats, which may be related to the regulation of SIRT1/JNK signaling pathway.

Conclusion: In conclusion, AM and CZ significantly reduced renal fibrosis and inflammation in CKD rats, which may be related to the regulation of SIRT1/JNK signaling pathway. Furthermore, L-Threonine, D-pantothenic acid, and nicotinamide may be potential biomarkers for the progression and treatment of CKD.

KEYWORDS

Astragalus membranaceus, *Curcuma zedoaria*, chronic kidney disease, metabolomic, SIRT1/JNK signaling pathway

Introduction

Chronic kidney disease (CKD) is a progressive disease with a high mortality and morbidity rate. In 2017, there were 697.5 million cases of CKD globally, and the CKD mortality rate for all ages increased by 41.5% from 1990 to 2017 (Bikbov et al., 2020). According to WHO Global Health Estimates, kidney diseases are the world's 10th leading cause of death. Mortality has increased from 813,000 in 2,000 to 1.3 million in 2019. The burden of CKD is increasing worldwide. CKD is usually caused by diabetes and hypertension (Kalantar-Zadeh et al., 2021). Optimal management of CKD involves reducing cardiovascular risk, treating albuminuria, avoiding nephrotoxins, and adjusting drug dosage (Chen et al., 2019). Even though treatment methods such as the angiotensin converting enzyme inhibitor (ACEI) or angiotensin receptor blocker (ARB) are available (Inker et al., 2014) and, more recently, a sodium-glucose cotransporter 2 (SGLT2) (Cherney et al., 2020; Heerspink et al., 2020) for the treatment of diabetic and non-diabetic CKD patients, risk of CKD progression remains high (Perkovic et al., 2019), and new therapies are needed.

Traditional Chinese Medicine (TCM) has been recognized as a potentially effective therapy for CKD (Zhong et al., 2013; Deng et al., 2020; Xu et al., 2021). *Astragalus membranaceus* (AM) has been clinically applied to treat CKD for several years due to its immunosuppressive, anti-fibrotic, and anti-inflammatory properties (Xu et al., 2016; Chen et al., 2020; Hu et al., 2020; Han et al., 2021). *Curcuma zedoaria* (CZ) has a potential to prevent and/or manage various diseases due to its anti-inflammatory, antioxidant, and anti-apoptotic properties (White et al., 2019; Alvarenga et al., 2020; Patel et al., 2020). Couplet medicines, one of the unique characteristics of TCM, are a combination of two single herbs used in tandem to treat a specific disease to increase effectiveness or minimize side effects (Chan, 1995). The combination of AM and CZ has been widely

used in the treatment of CKD in TCM, but their combination mechanism is not clear.

Metabonomics has emerged as an important technology to understand the pathophysiology, molecular mechanism and identify diagnosis and prognosis of various diseases (Kalantari and Nafar, 2019). Metabolomics has been increasingly used in exploring biomarkers and mechanisms of CKD (Wang et al., 2019; Dubin and Rhee, 2020; Hunter et al., 2021). In this study, we undertook a metabolomics analysis to explore the metabolic profiles and identify potential biomarkers in CKD rats with AM and CZ treatment.

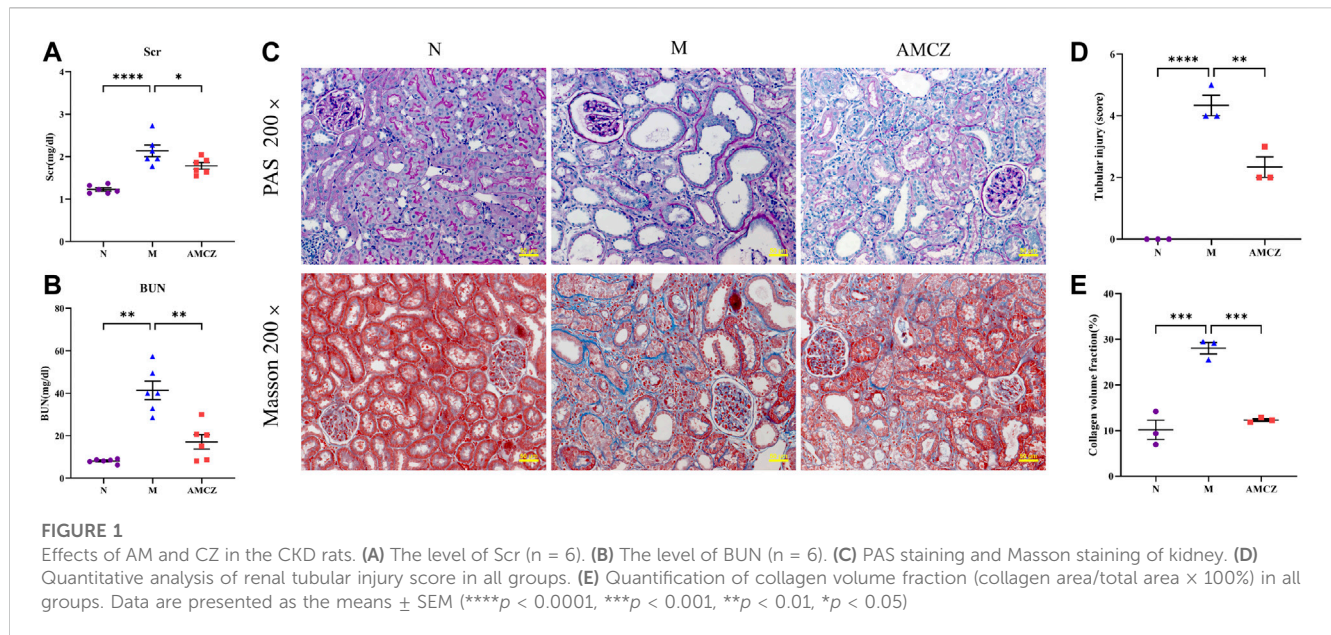
Materials and methods

Materials and reagents

AM and CZ were bought from Guangdong E-Fong Pharmaceutical (Guangdong, China). AM and CZ were standardized to 10 g per bag. They were prepared into a liquid of 1.87 g/mL for intragastric administration. Adenine was obtained from Yuan-ye (Shanghai, China). L-Threonine, D-pantothenic acid, nicotinamide were obtained from Zzstandard (Shanghai, China). Acetonitrile and Methanol were bought from CNW Technologies GmbH (Düsseldorf, Germany). Creatinine Serum Detection Kit and Blood Urea Nitrogen Detection Kit were bought from StressMarq Biosciences (British Columbia, Canada).

Animals

Male 8-weeks-old Sprague-Dawley (SD) rats (n = 18) were purchased from Guangdong Medical Laboratory Animal Center



(Foshan, China, permitted by SCXK,2013-0002 [YUE]). All rats were placed in a facility with fixed temperature (22°C–24°C) and relative humidity (50%–70%) with 12 h light/dark cycle. After 7 days of adaptive feeding, all rats were randomly divided into three groups: normal group (N, n = 6), model group (M, n = 6), and AM and CZ group (AMCZ, n = 6). Addition of 0.75% adenine to the diet of rats for 3 weeks induced the animal model of CKD (Yokozawa et al., 1986; Diwan et al., 2018). The AMCZ was administered AM and CZ (2.1 g/kg/d) by gastric irrigation for 4 weeks. The rats were sacrificed at the end of the experiment, All rats were anesthetized, and blood samples were taken from the abdominal aorta. Kidney samples were collected for further analysis.

Biochemical analysis

Creatinine Serum Detection Kit (StressMarq Biosciences, British Columbia, Canada) and Blood Urea Nitrogen Detection Kit (StressMarq Biosciences, British Columbia, Canada) were used to measure serum creatinine (SCR) and blood urea nitrogen (BUN).

Histological analysis

Kidneys were fixed in 4% paraformaldehyde for 24 h and embedded in paraffin. Periodic-acid-Schiff (PAS) staining was performed to evaluate renal pathological injury. Masson staining was used to estimate renal fibrosis. The tubular injury score was calculated using PAS staining and was based on the atrophy, shedding, and tubular dilation of tubular epithelial cells. The scoring system was as follows: 0 = no tubular injury; 1 = <10%; 2 = 10–25%; 3 = 26–50%; 4 = 51–75%; and 5 = >75% tubular injury (Wei et al., 2022). We used ImageJ software (National Institutes of Health, United States) to evaluate tubular interstitial fibrosis in Masson staining. Collagen volume fraction was calculated as follows: collagen area/total area × 100%.

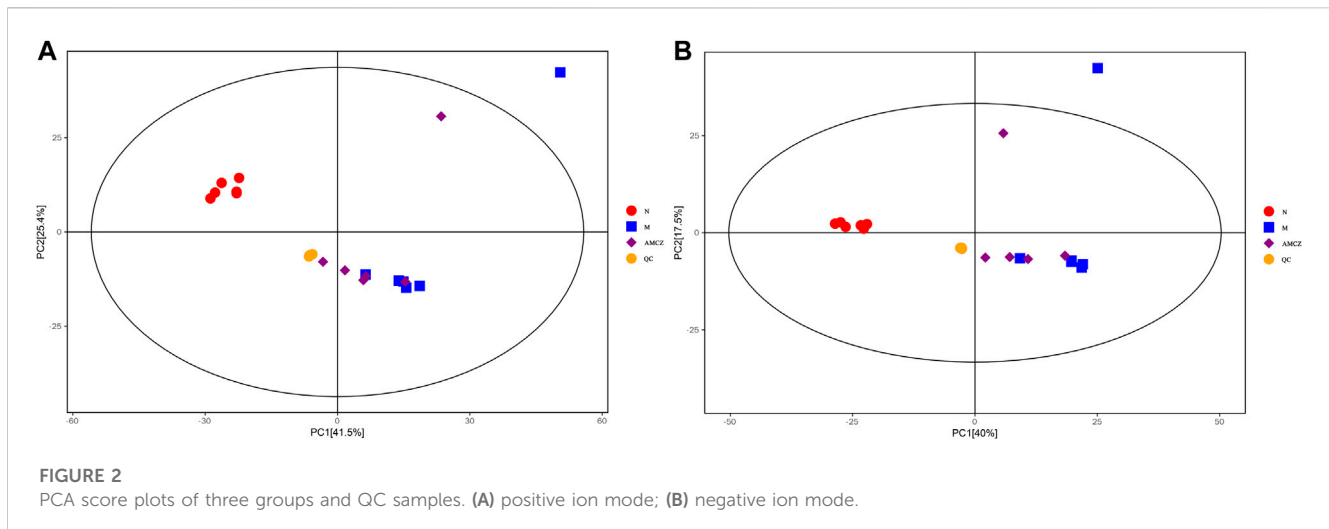
UHPLC-QE-MS based untargeted metabolomics analysis

The samples were extracted by 500 µL extraction solution (methanol/acetonitrile/water, 2:2:1, with isotopically-labelled internal standard mixture). After the centrifugation (12,000 r/min, 4°C, 15 min), supernatant was transferred into the liquid vial for metabolomics analysis. In order to guarantee the stability and repeatability of the ultra-high-performance liquid chromatography-tandem mass spectrometry (UHPLC-MS/MS) system, we prepared quality control (QC) samples by mixing equal aliquots of the supernatants from each group in the manner described above. The QC samples were staggered with the other samples (after every six samples).

We performed liquid chromatography/tandem mass spectrometry (LC-MS/MS) analysis using a UHPLC system (Vanquish, Thermo Fisher Scientific) coupled to a Q Exactive HFX mass spectrometer (Orbitrap MS, Thermo). The mobile phase consisted of 25 mmol/L ammonium acetate and 25 ammonia hydroxide in water (pH = 9.75) (A) and acetonitrile (B). The acquisition software continuously evaluates the MS spectrum in this mode. ESI source conditions were set as follows: sheath gas flow rate was 30 Arb, aux gas flow rate was 25 Arb, capillary temperature was 350°C, full MS resolution was 60,000, MS/MS resolution was 7,500, collision energy was 10/30/60 in NCE mode, and spray voltage was 3.6 kV (positive) or –3.2 kV (negative).

Data processing, multivariate data analysis and biomarker identification

The raw data were converted to the mzXML format then using Proteo Wizard and processed with an in-house program, which was developed using R and based on XCMS, for peak detection, extraction, alignment, and integration. After that, an in-house MS2 database (BiotreeDB) was applied to the annotation of metabolites. The cutoff for annotation was set at 0.3. SIMCA software (V15.0.2, Sartorius Stedim Data Analytics AB, Umea, Sweden) was utilized for principal



component analysis (PCA) and orthogonal partial least squares discriminant analysis (OPLS-DA). The metabolites with variable importance in projection (VIP) > 1 (OPLS-DA) and $p < 0.05$ (Student's *t*-test) were considered as significantly changed metabolites. Additionally, pathway enrichment analyses were conducted using biochemical databases including KEGG (<http://www.genome.jp/kegg/>) and MetaboAnalyst (<http://www.metaboanalyst.ca/>).

UHPLC-MRM-MS/MS analysis

The samples were extracted by 500 μ L extraction solution (methanol/acetonitrile/water, 2:2:1, precooling at -40°C). The upon mixture was vortexed for 30s and sonicated for 5 min at 0°C , followed by homogenization for 4 min at 40 Hz. The homogenate and sonicate cycle was repeated three times. After the above procedure, the sample was incubated at -40°C for an hour and centrifuged at 12,000 rpm for 15 min at 4°C . The UHPLC separation was carried out using an ExionLC-Sciex (Sciex), equipped with a Waters ACQUITY UPLC BEH Amide (100 \times 2.1 mm, 1.7 μm , Waters). The mobile phase A was 5 mM ammonium acetate & 0.1% acetic acid in water, and the mobile phase B was acetonitrile. A SCIEX 6500 QTRAP + triple quadrupole mass spectrometer (Sciex), equipped with an IonDrive Turbo V electrospray ionization (ESI) interface, was applied for assay development. Typical ion source parameters were: Curtain Gas = 40 psi, IonSpray Voltage = ± 4500 V, temperature = 475°C , Ion Source Gas 1 = 30 psi, Ion Source Gas 2 = 30 psi. The MRM parameters for each of the targeted analytes were optimized using flow injection analysis and were performed by injecting the standard solutions of the individual analytes into the API source of the mass spectrometer. SCIEX Analyst Work Station Software (Version 1.6.3) and Sciex MultiQuantTM 3.0.3 were employed for MRM data acquisition and processing.

Western blotting

The cortex tissues of the kidneys were lysed with RIPA lysis buffer. The proteins were separated by electrophoresis, and the proteins on the SDS-polyacrylamide gel were transferred to a polyvinylidene difluoride membrane (Millipore, United States). Following blocking in 5% non-fat

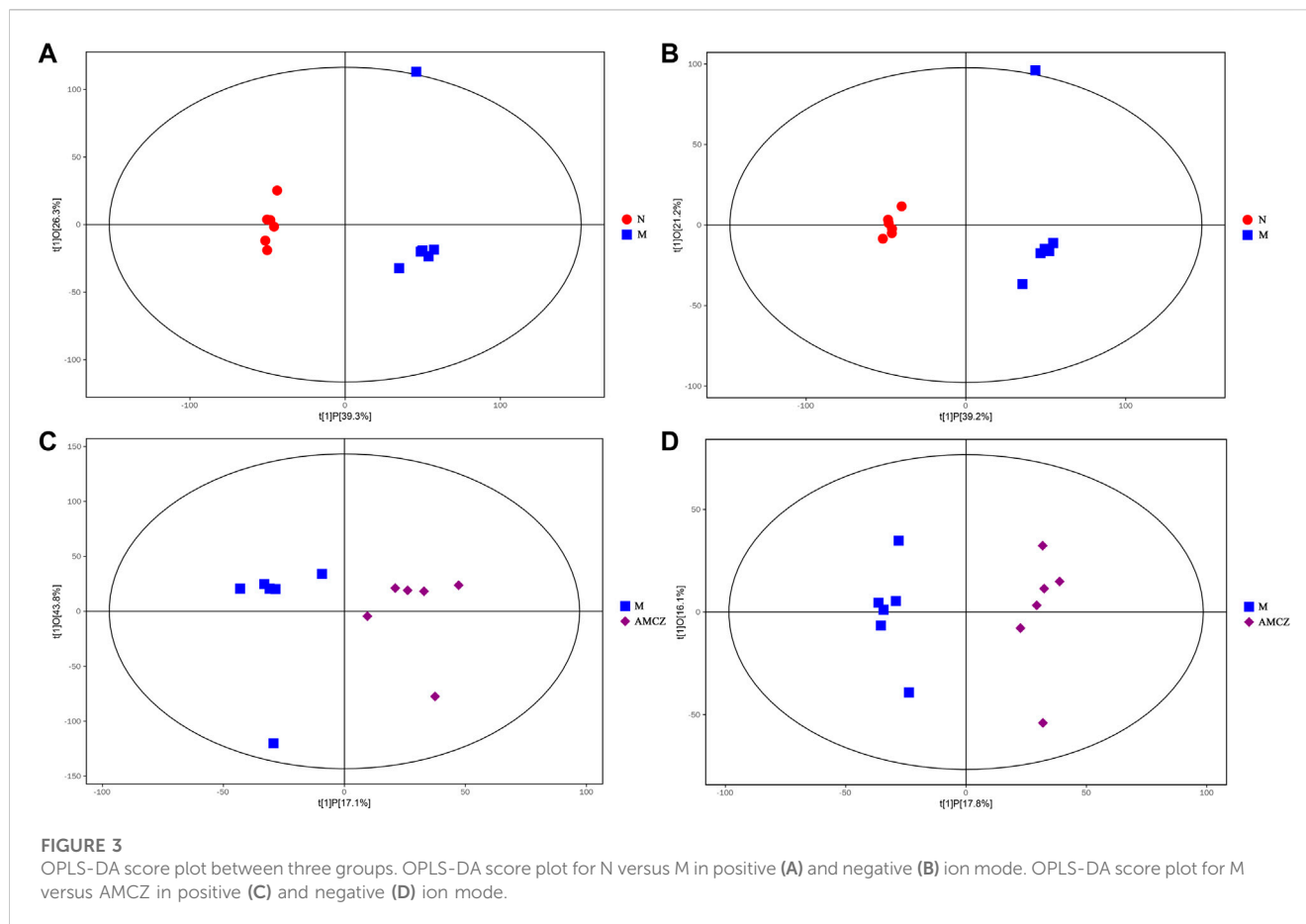
milk for 1 h at room temperature, the membranes were incubated with various primary antibodies at 4°C overnight. The primary antibodies included SIRT1(1:1000, proteintech), p-JNK(1:1000, proteintech), JNK(1:1000, proteintech), Fibronectin (FN) (1:1,000, Abcam), Collagen IV(Col-IV) (1:500, Abcam), α -SMA (1:500, Sigma), GAPDH (1:1,000, Cell Signaling Technology). Then, the membranes were incubated in HRP-conjugated secondary antibodies for 1 h at room temperature. HRP activity was visualized using Tanon-6100C.

Real-time reverse transcription polymerase chain reaction (RT-PCR) assay

Total RNA from the cortex tissues was extracted using RNA Isolation Kit V2 (Vazyme, China), and cDNA was synthesised using the HiScript II Q RT SuperMix for qPCR (+gDNA wiper) (Vazyme, China), according to the manufacturer's instructions. Real-time RT-PCR was carried out on the cDNA samples using ChamQ Universal SYBR qPCR Master Mix (Vazyme, China). The sequences of primers were as follows: IL-1 β forward, 5'-AGCTCTCCACCTCAATGGAC-3' and reverse, 5'-TTGTTTGGGATCCACACTCTCC-3', TNF- α forward, 5'-ATGGGCTCCCTCTCATCAGTTC-3' and reverse, 5'-CCTCCGCTTGGTGGTTTGCTAC-3', β -actin forward, 5'-GTGAAAAGATGACCCAGGACT-3' and reverse, 5'-TCTCATCTGGGAAAGAGCAGAA-3'. All amplifications were carried out in triplicate and repeated three times. The PCR data were analysed using the CFX Connect Real-Time PCR System (Bio-Rad, United States). Cycle threshold (CT) values were analysed using the comparative CT ($\Delta\Delta\text{CT}$) method, and the relative amount of target mRNA ($2^{-\Delta\Delta\text{CT}}$) was obtained by normalising to endogenous β -actin levels.

Statistical analysis

All quantitative were presented as the mean \pm SEM. All statistical analyses were performed using GraphPad Prism version 8.0.0 for Windows (GraphPad Software, San Diego, California United States). Statistically significant differences were determined by one-way ANOVA followed by Tukey's



multiple comparisons test. Brown-Forsythe and Welch ANOVA tests when variances are unequal. If the data does not follow a normal distribution, use the Kruskal-Wallis test. Statistical significance was considered at $p < 0.05$.

Results

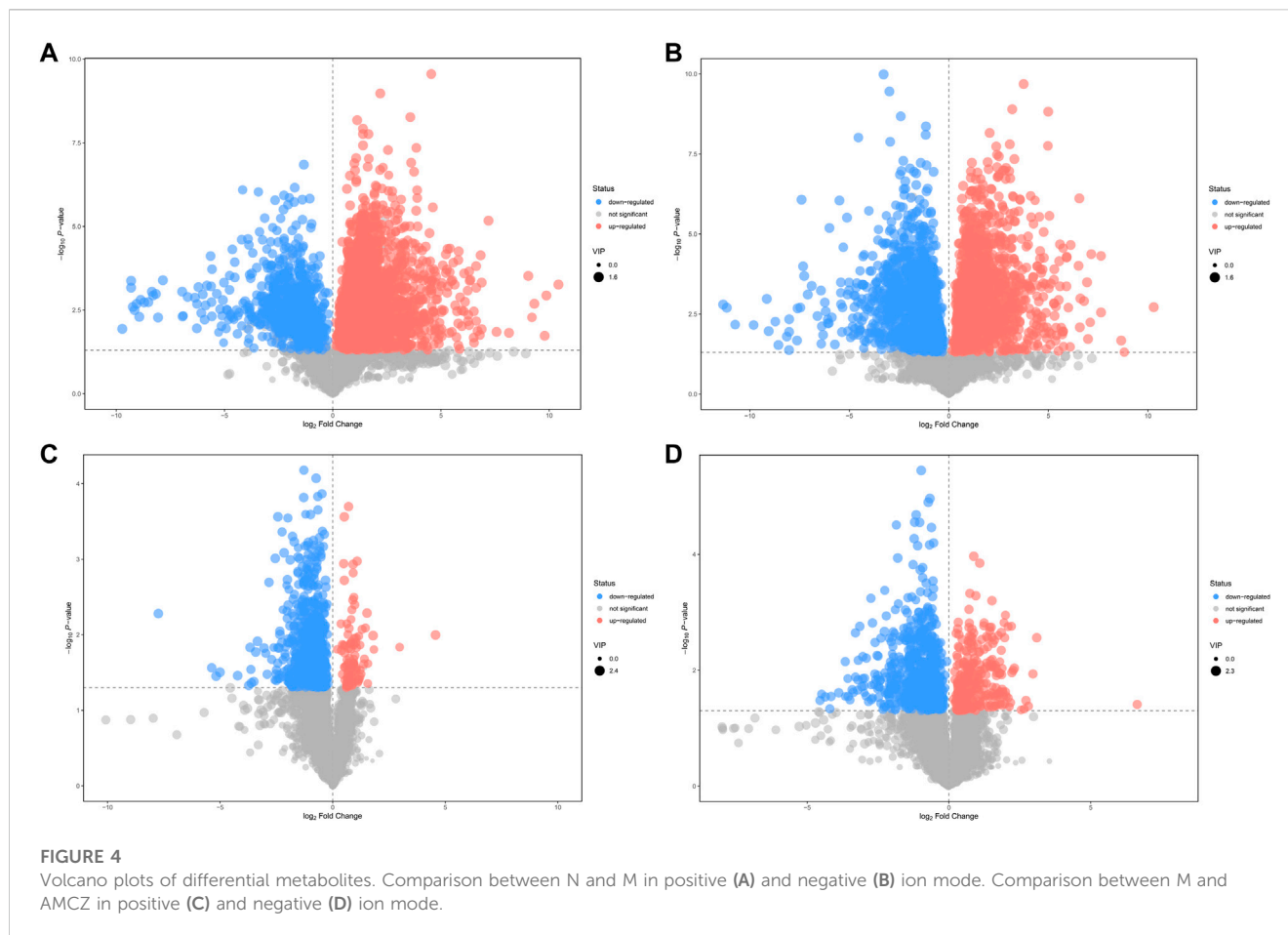
AM and CZ ameliorated renal injury in CKD rat

The levels of Scr and BUN were significantly increased in model group relative to normal group. This increase was reversed by AM and CZ treatment of the CKD rats (Figures 1A, B). Furthermore, Periodic Acid-Schiff (PAS) staining and Masson staining showed obvious features of CKD, such as tubular atrophy, interstitial fibrosis, and this was significantly inhibited by AM and CZ in CKD rats (Figures 1C-E).

UHPLC-QE-MS analysis and multivariate analysis of UHPLC-QE-MS data

UHPLC-QE-MS was used to analyze the kidney samples of normal group (N), model group (M), and AM and CZ group (AMCZ), and data acquisition was performed in positive and

negative ion modes. QC samples were used to confirm the reliability of the analytical method, the extracted ion chromatogram (EIC) of QC samples are shown in Supplementary Figure S1. PCA, an unsupervised analysis that reduces the dimensions of data, was applied to visualize the distribution and grouping of the samples. To identify potential outliers in the dataset, the 95% confidence interval in the PCA score plot was used as the threshold. In the PCA of all the samples, we found that QC samples were closely clustered together, which indicated the reliability and stability of the data (Figures 2A, B) and that the obtained data could be used for subsequent metabolomics research. PCA was performed to investigate whether the three groups could be separated and to reveal their metabolic distinctions. As shown in Figures 2A, B, there were distinctly separated clusters between the N, M, and AMCZ groups in both positive ion mode and negative ion mode. A similar finding was also found in the score plots of OPLS-DA, a more reliable pattern recognition method that was carried out to sharpen the separation among groups (Figures 3A-D). In order to examine the robustness and predictive abilities of the OPLS-DA model, 200 permutations were conducted. Then, we obtained the R^2 and Q^2 intercept values. R^2 indicates how well a variable's variation could be explained, whereas Q^2 indicates how well a variable could be predicted. The intercept value of Q^2 represents the robustness of the model, the risk of overfitting, and the degree of reliability of the model. The smaller the intercept of Q^2 , the stronger the robustness (Supplementary Figure S2).

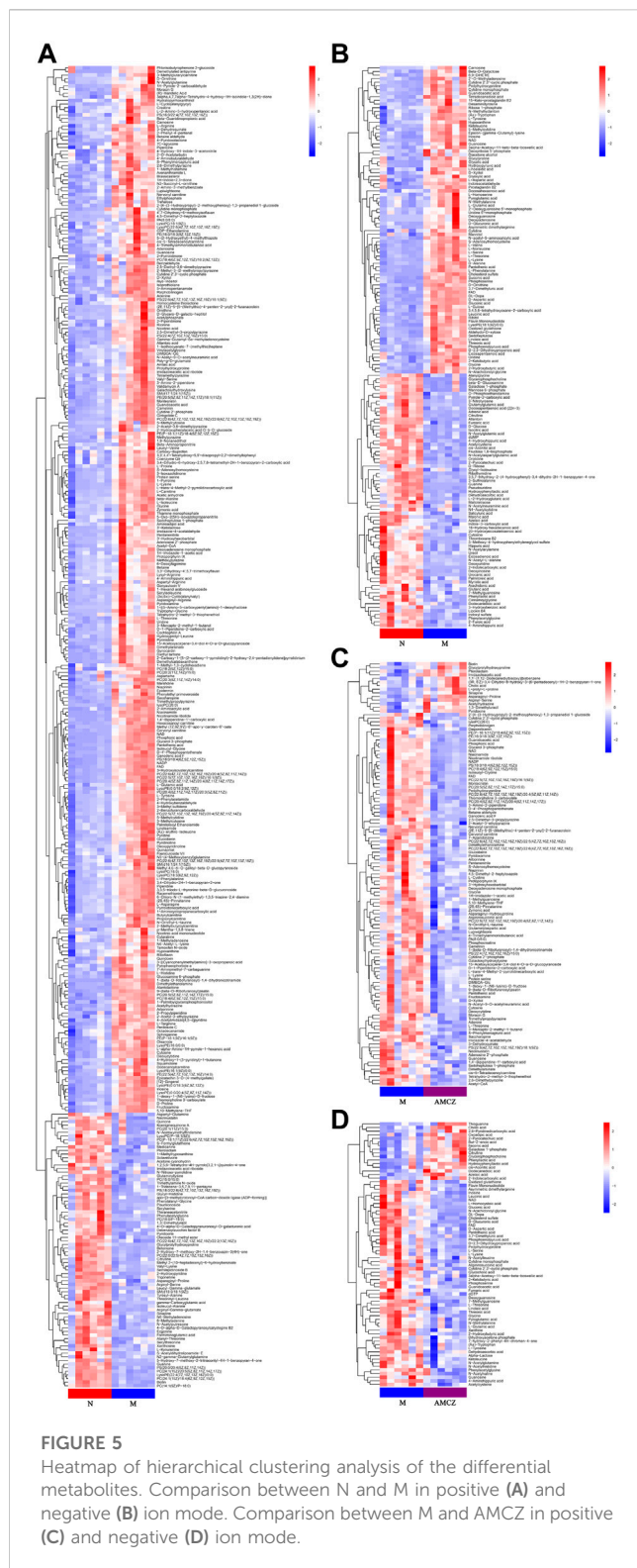


Identification of potential biomarkers

A value of variable importance in the projection (VIP) of the first principal component of an OPLS-DA analysis was determined. It indicates the importance of each variable in the model. The metabolites with $VIP > 1$ and $p < 0.05$ were considered as significantly changed metabolites. We visualized and filtered differential metabolites utilizing OPLS-DA mode in the volcano plots (Figure 4). Between N and M group, 365 and 155 metabolites with significant differences were identified under positive ion mode and negative ion mode, respectively (Supplementary Tables S1, S2). In addition, under positive ion mode and negative ion mode, 117 and 73 metabolites with significantly different expressions were identified between M and AMCZ respectively (Supplementary Tables S3, S4).

Hierarchical clustering analyses and correlation analysis of differential metabolites were shown in Figures 5, 6. Based on the Spearman correlation analysis, the metabolites classification and source were shown by chord diagram. The differential metabolites classification and source between three groups included lipids and lipid like molecules, organoheterocyclic compounds, organic acids and derivatives, nucleosides, nucleotides and analogues, organic acids and derivatives, etc., (Figure 7). Furthermore, we used commercial databases including KEGG (<http://www.genome.jp/>

[kegg/](http://www.genome.jp/kegg/)) and MetaboAnalyst (<http://www.metaboanalyst.ca/>) for pathway enrichment analysis. In positive ion mode, the main metabolic pathways significantly affected by CKD included histidine metabolism, nicotinate and nicotinamide metabolism, arginine and proline metabolism, glycine, serine and threonine metabolism, aminoacyl-tRNA biosynthesis, nitrogen metabolism, phenylalanine metabolism, methane metabolism, phenylalanine, tyrosine and tryptophan biosynthesis, and D-Glutamine and D-glutamate metabolism (Figure 8A). In negative ion mode, the main metabolic pathways significantly affected by CKD included citrate cycle (TCA cycle), histidine metabolism, glyoxylate and dicarboxylate metabolism, glycine, serine and threonine metabolism, phenylalanine, tyrosine and tryptophan biosynthesis, alanine, aspartate and glutamate metabolism, biosynthesis of unsaturated fatty acids, D-Glutamine and D-glutamate metabolism, and linoleic acid metabolism (Figure 8B). In positive ion mode, the main metabolic pathways significantly affected by AM and CZ treatment included glycine, serine and threonine metabolism, nicotinate and nicotinamide metabolism, biotin metabolism, vitamin B6 metabolism, methane metabolism, fatty acid elongation in mitochondria, and fatty acid metabolism (Figure 8C). In negative ion mode, the main metabolic pathways significantly affected by AM and CZ treatment included alanine, aspartate and glutamate metabolism, glutathione



metabolism, cyanoamino acid metabolism, arginine and proline metabolism, glycine, serine and threonine metabolism, aminoacyl-tRNA biosynthesis, citrate cycle (TCA cycle), nitrogen metabolism, methane metabolism, phenylalanine, tyrosine and tryptophan biosynthesis, D-Glutamine and D-glutamate

metabolism, linoleic acid metabolism, ascorbate and aldarate metabolism (Figure 8D).

We obtained massive data through metabolomics. In order to obtain marker metabolites, we analyzed metabolomics in two different ways: up-down (upregulated in M and downregulated by treatment) and down-up (downregulated in M and upregulated by treatment). Furthermore, we screened L-Threonine, D-pantothenic acid, and nicotinamide as potential marker metabolites by using a random forest model. In order to observe the effects of AM and CZ on potential marker metabolites, UHPLC-MRM-MS/MS analysis was performed to determine the concentration of L-threonine, D-pantothenic acid, and nicotinamide (Figure 9). It was found that the concentration of L-Threonine, D-pantothenic acid, and nicotinamide were decreased in M group compared with N group ($p < 0.001$), and the concentration of L-Threonine, D-pantothenic acid had a significant increased was observed in AMCZ group compared with M group ($p < 0.05$) (Figure 9A). The concentration of D-pantothenic was increased in AMCZ group compared with M group, but there was no statistical difference.

Effects of AMCZ on SIRT1/JNK signaling pathway in CKD rats

Nicotinamide adenine dinucleotide (NAD^+), is a key signaling molecule that regulates intermediary metabolism. NAD^+ acts as a coenzyme in the redox reaction and serves as an important substrate of sirtuins (Sirts) (Verdin, 2015, 1). We further examined the activation of SIRT1/JNK signaling pathway in the kidneys of CKD rats with AMCZ. As shown in Figure 10A, B, compared with the N group, the expression of SIRT1 was significantly downregulated in M group ($p < 0.01$). AMCZ attenuated this trend ($p < 0.01$). Compared with the N group, the expression of p-JNK was significantly upregulated in M group ($p < 0.01$). This increase was reversed by AM and CZ treatment of the CKD rats ($p < 0.01$).

Effects of AMCZ in the regulation of inflammation in CKD rats

The dysregulated inflammation is an important mechanism in the development of CKD. SIRT1 and JNK phosphorylation have been demonstrated to be crucial in modulating inflammation (Papaconstantinou, 2019; Yang et al., 2022). To further detect the level of pro-inflammatory factors, qRT-PCR was performed to assess the expression of IL-1 β and TNF- α in cortex tissues. The results (Figure 10C) showed that expression of IL-1 β and TNF- α in the M group was higher than that in the N group ($p < 0.05$), while AMCZ administration reversed the increase ($p < 0.05$).

Effects of AMCZ on renal fibrosis in CKD rats

The increased expressions of FN, Col-IV and α -SMA are crucial signals of renal tubulointerstitial fibrosis in the CKD progression. Figure 10 displayed the anti-fibrotic effects of the AMCZ treatments. Compared with the M group, the expression of α -SMA was significantly downregulated by AMCZ ($p < 0.01$). As shown in Figure 10A, B, 3 weeks of adenine-administration resulted in a significantly increased expression of Col-IV and FN ($p < 0.01$). AMCZ attenuated this trend ($p < 0.05$).

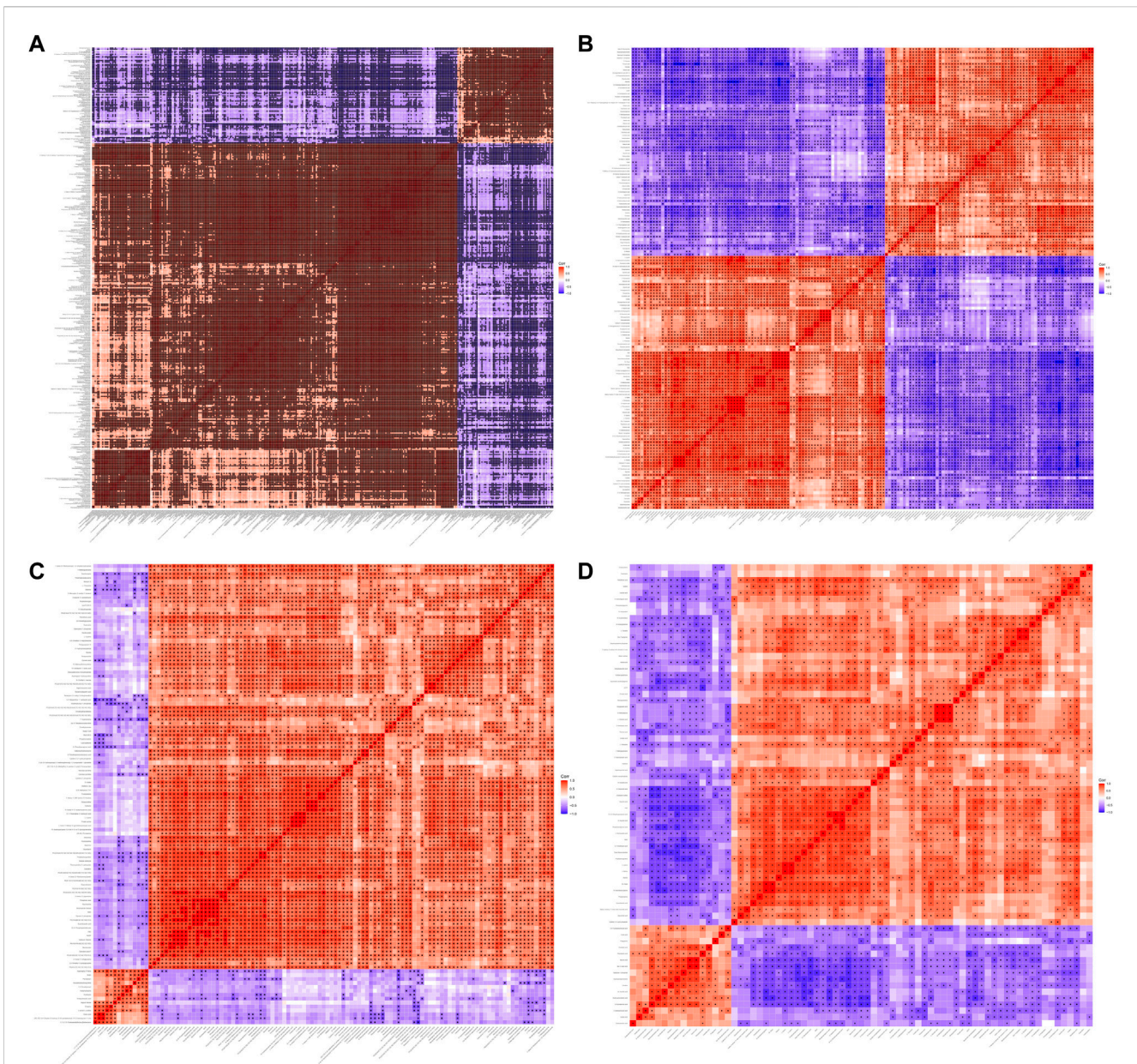


FIGURE 6

Heatmap of correlation analysis between three groups. Heatmap of correlation analysis N versus M in positive (A) and negative (B) ion mode. Heatmap of correlation analysis M versus AMCZ in positive (C) and negative (D) ion mode.

Discussion

In this study, we found histidine metabolism, nicotinate and nicotinamide metabolism, arginine and proline metabolism, glycine, serine and threonine metabolism were correlated with CKD pathophysiology. Additionally, we studied the effect and possible mechanisms of AM and CZ in the treatment of CKD, the results showed that AM and CZ alleviated adenine-induced kidney dysfunction, inflammation, and renal fibrosis, which are related to SIRT1/JNK signaling pathway. Furthermore, L-Threonine, D-pantothenic acid, and nicotinamide may be potential biomarkers for the progression and treatment of CKD.

As a progressive disease, CKD is characterized by dysfunctions in renal structure and function, which can be caused by various factors. Currently, the exact mechanism of CKD is still unclear (Lin et al., 2019). CKD progression may be attributed to parenchymal cell loss, microvascular damage, metabolic changes, oxidative stress, chronic inflammation, fibrosis, and reduced renal regeneration (Ruiz-Ortega et al., 2020). Studies have demonstrated that patients with CKD have significantly lower plasma histidine concentrations and negative correlations with pro-inflammatory markers (Watanabe et al., 2008), whereas histidine supplementation results in several health benefits, including anti-inflammatory, antioxidant, glucose-regulatory, and weight

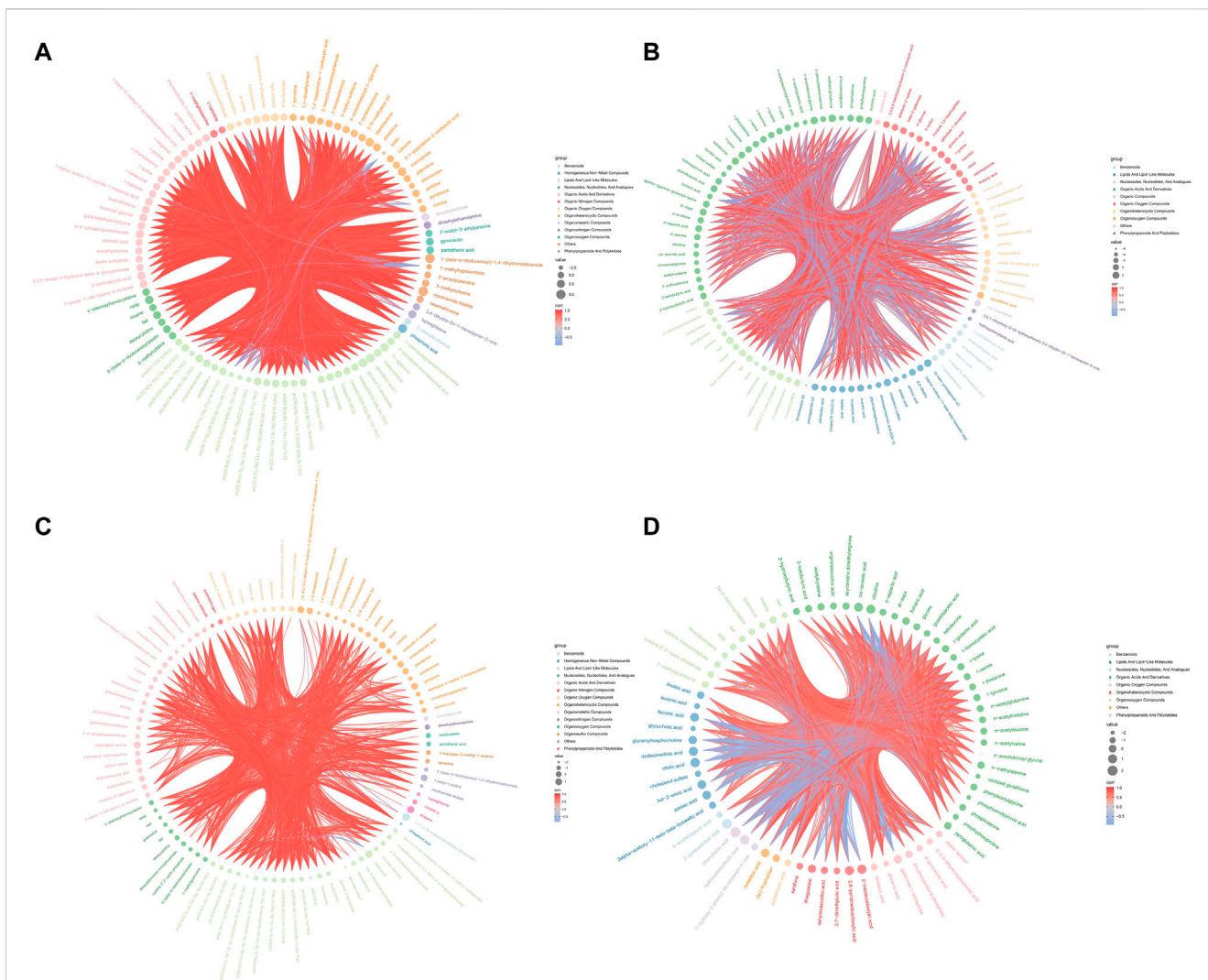
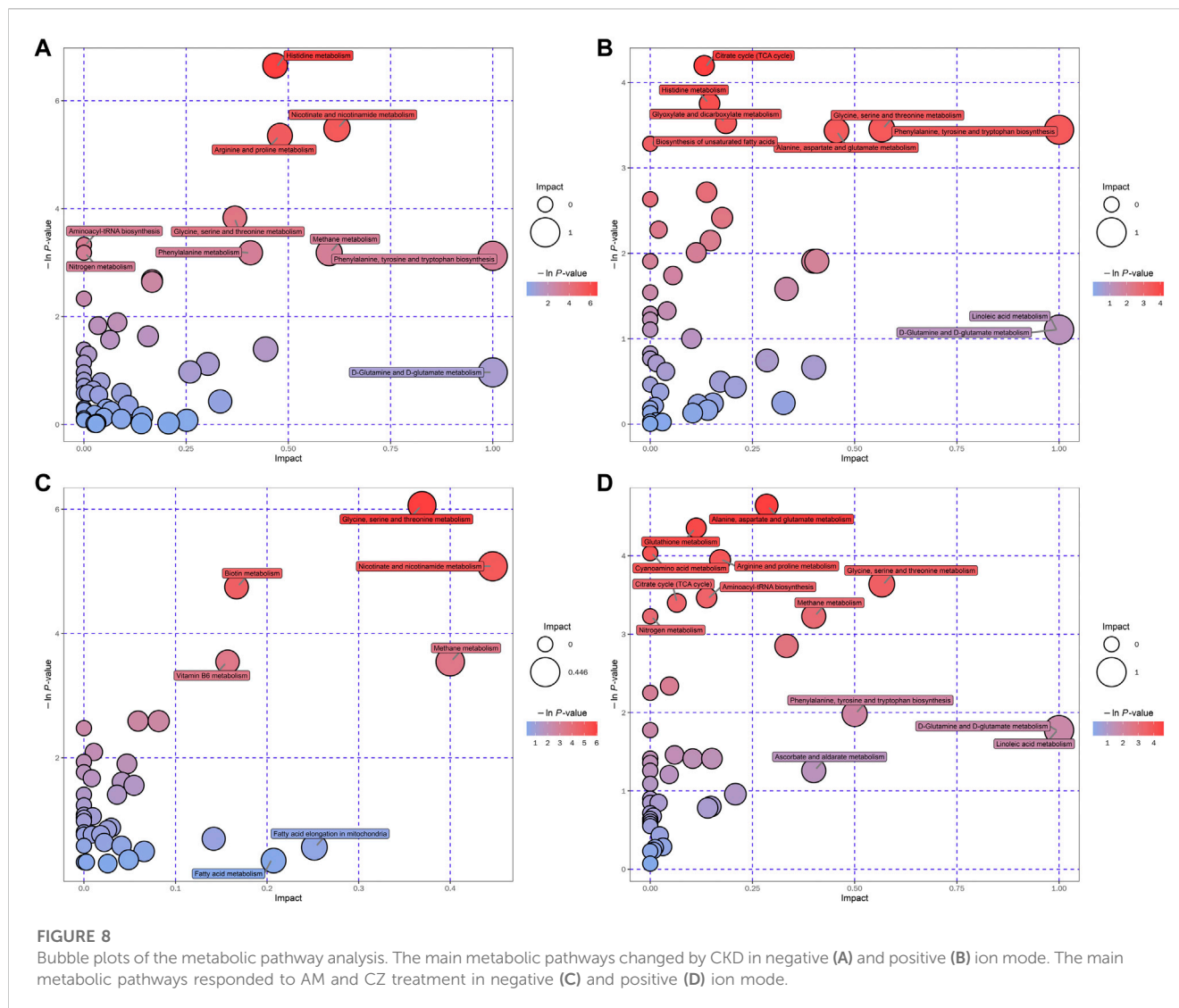


FIGURE 7 Chord diagram of spearman correlation analysis N versus M in positive (A) and negative (B) ion mode. Chord diagram of spearman correlation analysis the M versus AMCZ in positive (C) and negative (D) ion mode.

management (Holeček, 2020; Thalacker-Mercer and Gheller, 2020). Similarly, in our research, we found that L-histidine and L-glutamic acid were lower in the M group, and the expression of IL-1 β and TNF- α in the M group was higher than the N group. Histidine metabolism may be one of the main metabolic pathways significantly affected by CKD. Moreover, we found that nicotinamide metabolism (including nicotinamide adenine dinucleotide (NAD), nicotinamide adenine dinucleotide phosphate (NADP), niacinamide, and nicotinamide ribotide) was lower in the model group, which was similar to Zhu et al. (Zhu et al., 2021). Arginine is a semi-essential amino acid that is synthesized from glutamine, glutamate, and proline, and it is degraded by many pathways (Popolo et al., 2014). One of these breakdown mechanisms is the conversion of arginine to urea and ornithine. Additionally, arginine can be metabolized to nitric oxide (NO) and citrulline in the cytosol by nitric oxide synthetase (NOS). It has been reported that

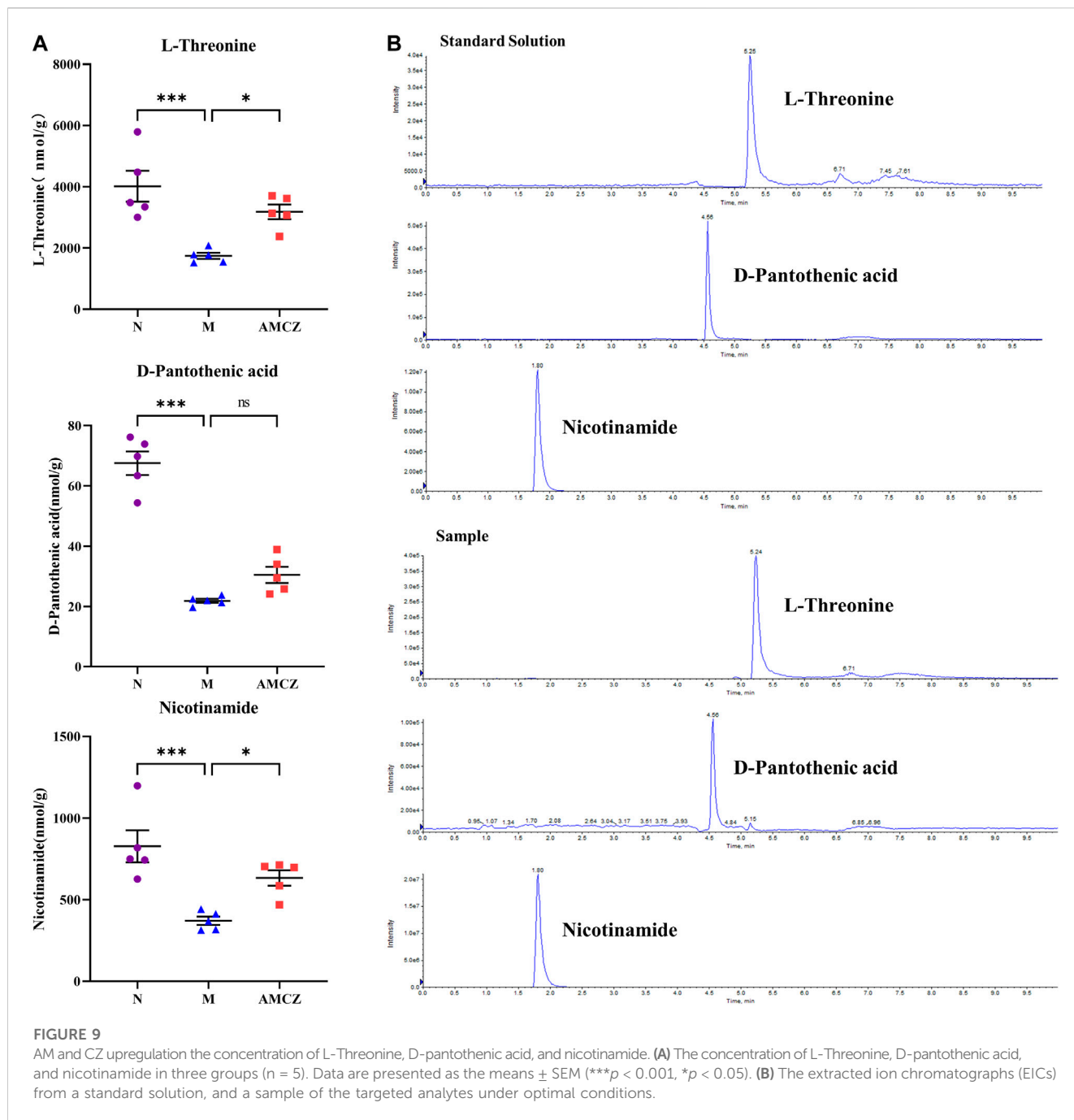
CKD patients produce less NO (Wever et al., 1999). In this study, we found D-proline and L-proline were lower in the CKD group.

There was a report that streptozotocin-induced diabetic mice have increased levels of urinary glycine (Hyeon et al., 2020), and elevated glycine levels in the urine are as a marker of tubular damage in rats (Wen et al., 2011). Glycine is the simplest amino acid, and its tiny size allows it to pass through the glomerular filtrate barrier. There is considerable resorption of this substance by the proximal tubules, and it is only detected in trace amounts in normal urine. Feng et al. (Feng et al., 2019) found serum glycine, cinnamoylglycine, and phenylacetylglycine were increased in CKD rats and renal function decline was associated with glycine metabolism. However, we found renal glycine levels were lower in CKD rats, but cinnamoylglycine and phenylacetylglycine levels were higher. This could be different from the test samples, therefore more research is needed.



We observed that levels of Scr and BUN, which were elevated in CKD, decreased after AM and CZ administration. Glycine, serine, and threonine metabolism and nicotinate and nicotinamide metabolism exhibited the greatest response to AM and CZ. Interestingly, Nicotinate and nicotinamide metabolism, and Glycine, serine and threonine metabolism were identified in both N versus M and M versus AMCZ groups. Moreover, we found that the concentration of nicotinamide was decreased in M group compared with N group, and an increased was observed in AMCZ group measured by UHPLC-MRM-MS/MS analysis. Nicotinamide, a vitamin B3 amide and precursor of nicotinamide adenine dinucleotide (NAD⁺), is a powerful antioxidant that may substantially minimize the damage produced by reactive oxygen species (ROS) in cells under oxidative stress (Mejía et al., 2018). Using UHPLC-MS/MS analysis, we found that in the M group, levels of 1-(beta-D-ribofuranosyl)-1, 4-dihydronicotinamide were significantly decreased, but they increased following administration of AM and CZ. 1-(beta-D-

ribofuranosyl)-1, 4-dihydronicotinamide, a reduced form of nicotinamide riboside, is considered to be a precursor to NAD⁺ (Bogan and Brenner, 2008). NAD⁺ serves as a substrate of SIRT1 and regulates SIRT1 expression (Mouchiroud et al., 2013). It has been demonstrated that NAD⁺ levels and SIRT1 activity can be effectively increased by administering NAD⁺ precursors such as nicotinamide mononucleotide (Yoshino et al., 2011) and nicotinamide riboside (Cantó et al., 2012). It has been reported that nicotinamide is involved in the regulation of inflammation (Weiss et al., 2015; Zheng et al., 2019). SIRT1 and JNK phosphorylation have been demonstrated to be crucial in modulating inflammation. In the present study, we found that the low expression of 1-(beta-D-ribofuranosyl)-1,4-dihydronicotinamide, nicotinamide, and SIRT1 was improved by the AMCZ treatment. AMCZ markedly lowered the elevated levels of p-JNK, FN, Col-IV, α -SMA, IL-1 β , and TNF- α in CKD rats, suggesting AMCZ attenuated renal fibrosis and inflammation through the modulation of SIRT1/JNK signaling pathway.



Besides, D-pantothenic acid is another potential marker worthy of attention. It has been proposed that pantothenic acid could be a potential biomarker for CKD progression. Furthermore, pantothenic acid is being used as a biomarker of albuminuria in normoalbuminuric hypertensive patients and has also been shown to be a promising biomarker for predicting diabetes-induced kidney impairment (Gonzalez-Calero et al., 2016; Ma et al., 2020). In addition, pantothenic acid is a potential therapeutic target for DN treatment (Daugherty et al., 2002; Demirci et al., 2014). Here, we showed that the concentration of D-pantothenic acid were decreased in M group

compared with N group, and an increased were observed in AMCZ group, suggesting that D-pantothenic acid were one of renal protective mechanisms.

Notably, L-threonine, an essential amino acid in both humans and animals, was decreased in CKD and returned to control levels in response to AM and CZ. Pathway enrichment analysis showed that Glycine, serine and threonine metabolism might be related to the occurrence and development of CKD. Recent research found that L-threonine can reduce inflammatory cytokine expression (Wang et al., 2021). L-threonine could potentially play a role in the detection and treatment of CKD. However, few

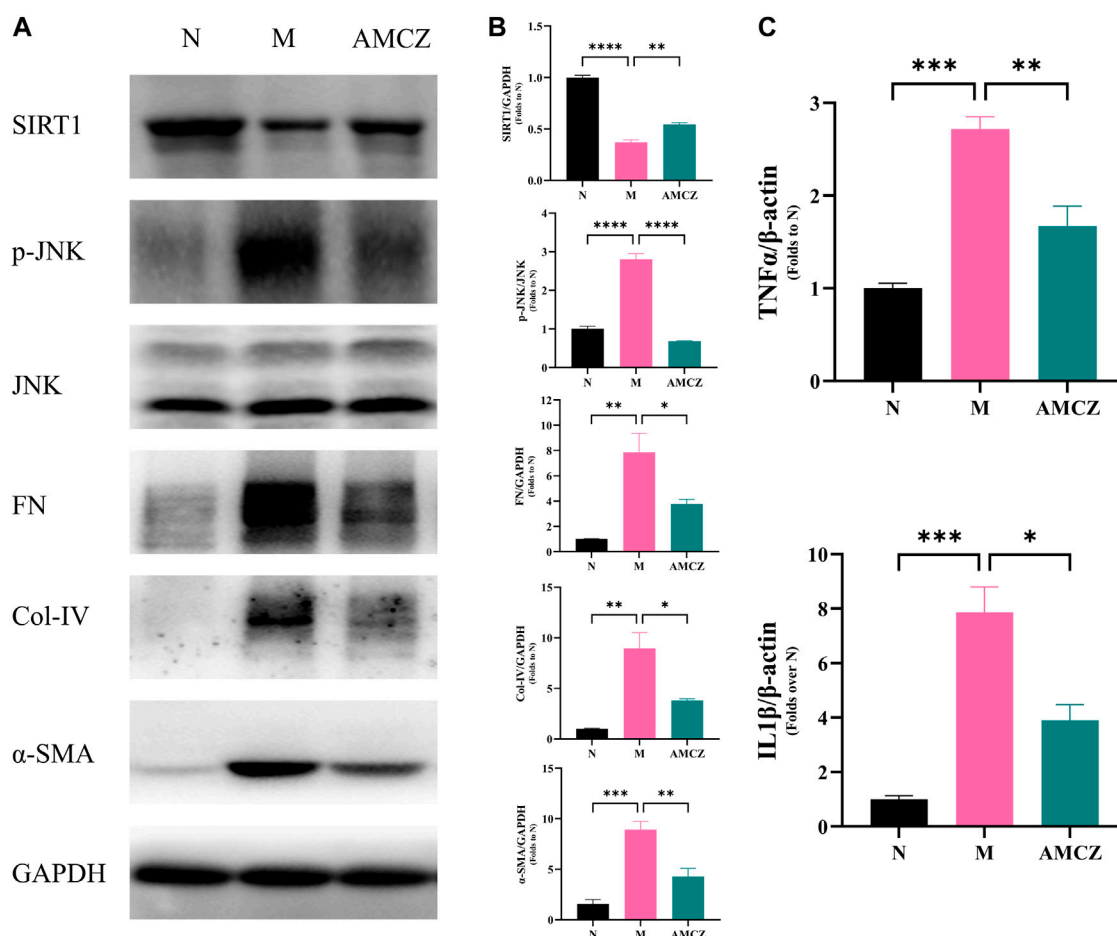


FIGURE 10

Effects of AM and CZ on SIRT1/JNK signaling pathway in adenine-induced CKD rats. **(A)** Representative Western blot images of SIRT1, p-JNK, JNK, FN, Col-IV, and α -SMA expression in the kidneys of rats. **(B)** Densitometric analysis of SIRT1, p-JNK, JNK, FN, Col-IV, and α -SMA normalized to GAPDH content. Values are expressed as mean \pm SEM, $n = 3$ rats per group ($*p < 0.05$, $**p < 0.01$, $***p < 0.001$, and $****p < 0.0001$ between the indicated two groups). The total RNA was isolated and subjected to real time RT-PCR to analyze the products of pro-inflammatory cytokines, IL-1 β and TNF- α in cortex tissues treated with AM and CZ. β -actin was used as an internal control ($*p < 0.05$, $**p < 0.01$, and $***p < 0.001$ between the indicated two groups).

studies have examined the relationship between L-threonine and CKD.

Conclusion

In summary, our study revealed that after AM and CZ treatments, CKD rats experienced a slew of complex and serious metabolic disorders. In addition, we discovered significant differences in metabolism in CKD rats, including nicotinate and nicotinamide metabolism, arginine and proline metabolism, and glycine, serine, and threonine metabolism. Moreover, we found that AM and CZ significantly reduced renal fibrosis and inflammation in CKD rats, which may be related to the regulation of SIRT1/JNK signaling pathway. Furthermore, L-Threonine, D-pantothenic acid, and nicotinamide may be potential biomarkers for the progression and

treatment of CKD. In conclusion, the results described above may contribute to the identification of metabolic biomarkers and novel therapeutic strategies to prevent or delay the progression of CKD.

Data availability statement

The original contributions presented in the study are included in the article/Supplementary Material, further inquiries can be directed to the corresponding authors.

Ethics statement

The animal study was reviewed and approved by Ethics Committee of Shenzhen TOP Biotechnology Co., Ltd.

Author contributions

Material preparation, data collection and analysis were performed by LL and JL. The first draft of the manuscript was written by LL and JC. Animal experiment were performed by BW, HP, and JP. XL, FL, and GX designed the experiments and provided revisions and comments to the manuscript. All authors reviewed and approved the final manuscript.

Funding

This study was supported by Shenzhen Science and Technology Project (JCYJ20220531092201003) and Shenzhen Fund for Guangdong Provincial Highlevel Clinical Key Specialties.

Conflict of interest

The authors declare that the research was conducted in the absence of any commercial or financial relationships that could be construed as a potential conflict of interest.

Publisher's note

All claims expressed in this article are solely those of the authors and do not necessarily represent those of their affiliated organizations, or those of the publisher, the editors and the

reviewers. Any product that may be evaluated in this article, or claim that may be made by its manufacturer, is not guaranteed or endorsed by the publisher.

Supplementary material

The Supplementary Material for this article can be found online at: <https://www.frontiersin.org/articles/10.3389/fphar.2023.1103527/full#supplementary-material>

SUPPLEMENTARY FIGURE S1

The extracted ion chromatogram (EIC) of QC samples obtained from in positive (A) and negative (B) ion mode.

SUPPLEMENTARY FIGURE S2

Permutation test of OPLS-DA model for N versus M in positive (A) and negative (B) ion mode. Permutation test of OPLS-DA model for M versus AMCZ in positive (C) and negative (D) ion mode.

SUPPLEMENTARY TABLE S1

Significantly differentially expressed metabolites in the kidney of N versus M in positive ion mode.

SUPPLEMENTARY TABLE S2

Significantly differentially expressed metabolites in the kidney of N versus M in negative ion mode.

SUPPLEMENTARY TABLE S3

Significantly differentially expressed metabolites in M and AMCZ in positive ion mode.

SUPPLEMENTARY TABLE S4

Significantly differentially expressed metabolites in M and AMCZ in negative ion mode.

References

- Alvarenga, L., Salarolli, R., Cardozo, L. F. M. F., Santos, R. S., de Brito, J. S., Kemp, J. A., et al. (2020). Impact of curcumin supplementation on expression of inflammatory transcription factors in hemodialysis patients: A pilot randomized, double-blind, controlled study. *Clin. Nutr.* 39, 3594–3600. doi:10.1016/j.clnu.2020.03.007
- Bikbov, B., Purcell, C. A., Levey, A. S., Smith, M., Abdoli, A., Abebe, M., et al. (2020). Global, regional, and national burden of chronic kidney disease, 1990–2017: A systematic analysis for the global burden of disease study 2017. *Lancet* 395, 709–733. doi:10.1016/S0140-6736(20)30045-3
- Bogan, K. L., and Brenner, C. (2008). Nicotinic acid, nicotinamide, and nicotinamide riboside: A molecular evaluation of NAD⁺ precursor vitamins in human nutrition. *Annu. Rev. Nutr.* 28, 115–130. doi:10.1146/annurev.nutr.28.061807.155443
- Cantó, C., Houtkooper, R. H., Pirinen, E., Youn, D. Y., Oosterveer, M. H., Cen, Y., et al. (2012). The NAD(+) precursor nicotinamide riboside enhances oxidative metabolism and protects against high-fat diet-induced obesity. *Cell Metab.* 15, 838–847. doi:10.1016/j.cmet.2012.04.022
- Chan, K. (1995). Progress in traditional Chinese medicine. *Trends Pharmacol. Sci.* 16, 182–187. doi:10.1016/S0165-6147(00)89019-7
- Chen, T. K., Knicely, D. H., and Grams, M. E. (2019). Chronic kidney disease diagnosis and management: A review. *JAMA* 322, 1294–1304. doi:10.1001/jama.2019.14745
- Chen, Z., Liu, L., Gao, C., Chen, W., Vong, C. T., Yao, P., et al. (2020). Astragali radix (huangqi): A promising edible immunomodulatory herbal medicine. *J. Ethnopharmacol.* 258, 112895. doi:10.1016/j.jep.2020.112895
- Cherney, D. Z. I., Dekkers, C. C. J., Barbour, S. J., Catran, D., Abdal Gafor, A. H., Greasley, P. J., et al. (2020). Effects of the SGLT2 inhibitor dapagliflozin on proteinuria in non-diabetic patients with chronic kidney disease (DIAMOND): A randomised, double-blind, crossover trial. *Lancet Diabetes & Endocrinol.* 8, 582–593. doi:10.1016/S2213-8587(20)30162-5
- Daugherty, M., Polanuyer, B., Farrell, M., Scholle, M., Lykidis, A., de Crécy-Lagard, V., et al. (2002). Complete reconstitution of the human coenzyme A biosynthetic pathway via comparative genomics. *J. Biol. Chem.* 277, 21431–21439. doi:10.1074/jbc.M201708200
- Demirci, B., Demir, O., Dost, T., and Birincioglu, M. (2014). Protective effect of vitamin B5 (dexpantenol) on cardiovascular damage induced by streptozocin in rats. *Bratisl. Lek. Listy* 115, 190–196. doi:10.4149/bll_2014_040
- Deng, X., Jiang, N., Guo, L., Wang, C., Li, J., Liu, X., et al. (2020). Protective effects and metabolic regulatory mechanisms of shenyan fangshuai recipe on chronic kidney disease in rats. *Evidence-Based Complementary Altern. Med.* 2020, 5603243–5603313. doi:10.1155/2020/5603243
- Diwan, V., Brown, L., and Gobe, G. C. (2018). Adenine-induced chronic kidney disease in rats: Models of kidney diseases. *Nephrology* 23, 5–11. doi:10.1111/nep.13180
- Dubin, R. F., and Rhee, E. P. (2020). Proteomics and metabolomics in kidney disease, including insights into etiology, treatment, and prevention. *Clin. J. Am. Soc. Nephrol.* 15, 404–411. doi:10.2215/CJN.07420619
- Feng, Y.-L., Cao, G., Chen, D.-Q., Vaziri, N. D., Chen, L., Zhang, J., et al. (2019). Microbiome-metabolomics reveals gut microbiota associated with glycine-conjugated metabolites and polyamine metabolism in chronic kidney disease. *Cell Mol. Life Sci.* 76, 4961–4978. doi:10.1007/s00018-019-03155-9
- Gonzalez-Calero, L., Martin-Lorenzo, M., Martinez, P. J., Baldan-Martin, M., Ruiz-Hurtado, G., Segura, J., et al. (2016). Hypertensive patients exhibit an altered metabolism. A specific metabolite signature in urine is able to predict albuminuria progression. *Transl. Res.* 178, 25–37.e7. doi:10.1016/j.trsl.2016.07.003
- Han, C., Jiang, Y., Li, W., and Liu, Y. (2021). Astragalus membranaceus and Salvia miltiorrhiza ameliorates cyclosporin A-induced chronic nephrotoxicity through the “gut-kidney axis”. *J. Ethnopharmacol.* 269, 113768. doi:10.1016/j.jep.2020.113768
- Heerspink, H. J. L., Stefánsson, B. V., Correa-Rotter, R., Chertow, G. M., Greene, T., Hou, F.-F., et al. (2020). Dapagliflozin in patients with chronic kidney disease. *N. Engl. J. Med.* 383, 1436–1446. doi:10.1056/NEJMoa2024816
- Holeček, M. (2020). Histidine in health and disease: Metabolism, physiological importance, and use as a supplement. *Nutrients* 12, 848. doi:10.3390/nu12030848
- Hu, R., Wang, M., Liu, L., You, H., Wu, X., Liu, Y., et al. (2020). Calycosin inhibited autophagy and oxidative stress in chronic kidney disease skeletal muscle atrophy by regulating AMPK/SKP2/CARM1 signalling pathway. *J. Cell. Mol. Med.* 24, 11084–11099. doi:10.1111/jcmm.15514

- Hunter, E., Percival, B., Ahmad, Z., Chang, M.-W., Hunt, J. A., Tasker, S., et al. (2021). NMR-Based metabolomics associated with chronic kidney disease in humans and animals: A one health perspective. *Mol. Cell Biochem.* 476, 4133–4137. doi:10.1007/s11010-021-04222-1
- Hyeon, J. S., Jung, Y., Lee, G., Ha, H., and Hwang, G.-S. (2020). Urinary metabolomic profiling in streptozotocin-induced diabetic mice after treatment with losartan. *IJMS* 21, 8969. doi:10.3390/ijms21238969
- Inker, L. A., Astor, B. C., Fox, C. H., Isakova, T., Lash, J. P., Peralta, C. A., et al. (2014). KDOQI US commentary on the 2012 KDIGO clinical practice guideline for the evaluation and management of CKD. *Am. J. Kidney Dis.* 63, 713–735. doi:10.1053/j.ajkd.2014.01.416
- Kalantar-Zadeh, K., Jafar, T. H., Nitsch, D., Neuen, B. L., and Perkovic, V. (2021). Chronic kidney disease. *Lancet* 398, 786–802. doi:10.1016/S0140-6736(21)00519-5
- Kalantari, S., and Nafar, M. (2019). An update of urine and blood metabolomics in chronic kidney disease. *Biomarkers Med.* 13, 577–597. doi:10.2217/bmm-2019-0008
- Lin, T.-A., Wu, V. C.-C., and Wang, C.-Y. (2019). Autophagy in chronic kidney diseases. *Cells* 8, 61. doi:10.3390/cells8010061
- Ma, T., Liu, T., Xie, P., Jiang, S., Yi, W., Dai, P., et al. (2020). UPLC-MS-based urine nontargeted metabolic profiling identifies dysregulation of pantothenate and CoA biosynthesis pathway in diabetic kidney disease. *Life Sci.* 258, 118160. doi:10.1016/j.lfs.2020.118160
- Mejía, S. Á., Gutman, L. A. B., Camarillo, C. O., Navarro, R. M., Becerra, M. C. S., Santana, L. D., et al. (2018). Nicotinamide prevents sweet beverage-induced hepatic steatosis in rats by regulating the G6PD, NADPH/NADP⁺ and GSH/GSSG ratios and reducing oxidative and inflammatory stress. *Eur. J. Pharmacol.* 818, 499–507. doi:10.1016/j.ejphar.2017.10.048
- Mouchiroud, L., Houtkooper, R. H., Moullan, N., Katsyuba, E., Ryu, D., Cantó, C., et al. (2013). The NAD⁺/Sirtuin pathway modulates longevity through activation of mitochondrial UPR and FOXO signaling. *Cell* 154, 430–441. doi:10.1016/j.cell.2013.06.016
- Papaconstantinou, J. (2019). The role of signaling pathways of inflammation and oxidative stress in development of senescence and aging phenotypes in cardiovascular disease. *Cells* 8, 1383. doi:10.3390/cells8111383
- Patel, S. S., Acharya, A., Ray, R. S., Agrawal, R., Raghuvanshi, R., and Jain, P. (2020). Cellular and molecular mechanisms of curcumin in prevention and treatment of disease. *Crit. Rev. Food Sci. Nutr.* 60, 887–939. doi:10.1080/10408398.2018.1552244
- Perkovic, V., Jardine, M. J., Neal, B., Bompoint, S., Heerspink, H. J. L., Charytan, D. M., et al. (2019). Canagliflozin and renal outcomes in type 2 diabetes and nephropathy. *N. Engl. J. Med.* 380, 2295–2306. doi:10.1056/NEJMoa1811744
- Popolo, A., Adesso, S., Pinto, A., Autore, G., and Marzocco, S. (2014). L-Arginine and its metabolites in kidney and cardiovascular disease. *Amino Acids* 46, 2271–2286. doi:10.1007/s00726-014-1825-9
- Ruiz-Ortega, M., Rayego-Mateos, S., Lamas, S., Ortiz, A., and Rodrigues-Diez, R. R. (2020). Targeting the progression of chronic kidney disease. *Nat. Rev. Nephrol.* 16, 269–288. doi:10.1038/s41581-019-0248-y
- Thalacker-Mercer, A. E., and Gheller, M. E. (2020). Benefits and adverse effects of histidine supplementation. *J. Nutr.* 150, 2588S–2592S. doi:10.1093/jn/nxaa229
- Verdin, E. (2015). NAD⁺ in aging, metabolism, and neurodegeneration. *Science* 350, 1208–1213. doi:10.1126/science.aac4854
- Wang, C., Yang, Y., Gao, N., Lan, J., Dou, X., Li, J., et al. (2021). L-Threonine upregulates the expression of β -defensins by activating the NF- κ B signaling pathway and suppressing SIRT1 expression in porcine intestinal epithelial cells. *Food Funct.* 12, 5821–5836. doi:10.1039/D1FO00269D
- Wang, Y.-N., Ma, S.-X., Chen, Y.-Y., Chen, L., Liu, B.-L., Liu, Q.-Q., et al. (2019). Chronic kidney disease: Biomarker diagnosis to therapeutic targets. *Clin. Chim. Acta* 499, 54–63. doi:10.1016/j.cca.2019.08.030
- Watanabe, M., Suliman, M. E., Qureshi, A. R., Garcia-Lopez, E., Bárány, P., Heimbürger, O., et al. (2008). Consequences of low plasma histidine in chronic kidney disease patients: Associations with inflammation, oxidative stress, and mortality. *Am. J. Clin. Nutr.* 87, 1860–1866. doi:10.1093/ajcn/87.6.1860
- Wei, X., Wang, Y., Weng, J., Lao, Y., Deng, R., Lu, J., et al. (2022). Combination of perindopril erbumine and huangqi-danshen decoction protects against chronic kidney disease via sirtuin3/mitochondrial dynamics pathway. *Evidence-Based Complementary Altern. Med.* 2022, e5812105. doi:10.1155/2022/5812105
- Weiss, R., Schilling, E., Grahnert, A., Kölling, V., Dorow, J., Ceglarek, U., et al. (2015). Nicotinamide: A vitamin able to shift macrophage differentiation toward macrophages with restricted inflammatory features. *Innate Immun.* 21, 813–826. doi:10.1177/1753425915602545
- Wen, H., Yang, H.-J., Choi, M.-J., Kwon, H.-N., Kim, M.-A., Hong, S.-S., et al. (2011). Identification of urinary biomarkers related to cisplatin-induced acute renal toxicity using NMR-based metabolomics. *Biomol. Ther.* 19, 38–44. doi:10.4062/biomolther.2011.19.1.038
- Wever, R., Boer, P., Hijmering, M., Stroes, E., Verhaar, M., Kastelein, J., et al. (1999). Nitric oxide production is reduced in patients with chronic renal failure. *ATVB* 19, 1168–1172. doi:10.1161/01.ATV.19.5.1168
- White, C. M., Pasupuleti, V., Roman, Y. M., Li, Y., and Hernandez, A. V. (2019). Oral turmeric/curcumin effects on inflammatory markers in chronic inflammatory diseases: A systematic review and meta-analysis of randomized controlled trials. *Pharmacol. Res.* 146, 104280. doi:10.1016/j.phrs.2019.104280
- Xu, C., Tang, F., Lu, M., Yang, J., Han, R., Mei, M., et al. (2016). Pretreatment with Astragaloside IV protects human umbilical vein endothelial cells from hydrogen peroxide induced oxidative stress and cell dysfunction by inhibiting eNOS uncoupling and NADPH oxidase – ROS – NF- κ B pathway. *Can. J. Physiol. Pharmacol.* 94, 1132–1140. doi:10.1139/cjpp-2015-0572
- Xu, H., Wu, T., and Huang, L. (2021). Therapeutic and delivery strategies of phytoconstituents for renal fibrosis. *Adv. Drug Deliv. Rev.* 177, 113911. doi:10.1016/j.addr.2021.113911
- Yang, Y., Liu, Y., Wang, Y., Chao, Y., Zhang, J., Jia, Y., et al. (2022). Regulation of SIRT1 and its roles in inflammation. *Front. Immunol.* 13, 831168. doi:10.3389/fimmu.2022.831168
- Yokozawa, T., Zheng, P. D., Oura, H., and Koizumi, F. (1986). Animal model of adenine-induced chronic renal failure in rats. *Nephron* 44, 230–234. doi:10.1159/000183992
- Yoshino, J., Mills, K. F., Yoon, M. J., and Imai, S. (2011). Nicotinamide mononucleotide, a key NAD⁺ intermediate, treats the pathophysiology of diet- and age-induced diabetes in mice. *Cell Metab.* 14, 528–536. doi:10.1016/j.cmet.2011.08.014
- Zheng, M., Cai, J., Liu, Z., Shu, S., Wang, Y., Tang, C., et al. (2019). Nicotinamide reduces renal interstitial fibrosis by suppressing tubular injury and inflammation. *J. Cell Mol. Med.* 23, 3995–4004. doi:10.1111/jcmm.14285
- Zhong, Y., Deng, Y., Chen, Y., Chuang, P. Y., and Cijiang He, J. (2013). Therapeutic use of traditional Chinese herbal medications for chronic kidney diseases. *Kidney Int.* 84, 1108–1118. doi:10.1038/ki.2013.276
- Zhu, H., Cao, C., Wu, Z., Zhang, H., Sun, Z., Wang, M., et al. (2021). The probiotic L. casei Zhang slows the progression of acute and chronic kidney disease. *Cell Metab.* 33, 1926–1942.e8. doi:10.1016/j.cmet.2021.06.014